Tensile Cyclic Strength and Macroscopic Failure Characteristics of C/C and the Metal Impregnated C/C

Moriyama, Masahiro
Department of Aeronautics and Astronautics, Graduate School of Engineering, Kyushu University

Takao, Yoshihiro
Research Institute for Applied Mechanics, Kyushu University

Wang, Wen-Xue
Research Institute for Applied Mechanics, Kyushu University

Matsubara, Terutake
Research Institute for Applied Mechanics, Kyushu University

https://doi.org/10.15017/26792

出版情報：九州大学応用力学研究所所報. 129, pp.25-30, 2005-09. Research Institute for Applied Mechanics, Kyushu University
バージョン：
権利関係：

Tensile Cyclic Strength and Macroscopic Failure Characteristics of C/C and the Metal Impregnated C/C

Masahiro MORIYAMA[*1], Yoshihiro TAKAO[*2],
Wen-Xue WANG[*2] and Terutake MATSUBARA[*2]
E-mail of corresponding author: *ytakao@riam.kyushu-u.ac.jp*

(Received July 29, 2005)

Abstract

Tensile cyclic strength and macroscopic behavior of C/C and metal impregnated C/C composites such as Cu-C/C and Si-C/C were investigated experimentally. From the results of tensile-tensile cyclic loading tests, S-N curves of these materials were obtained and the fracture mechanism of these materials was discussed. The cyclic strength of metal impregnated C/C composites is about 80% of the ultimate tensile strength at $N=10^6$. Though strength degradation appears in low cycle region, the residual strength is increased in high cycle region.

Key words : *carbon-carbon (C/C); metal impregnated C/C; tensile cyclic loading; S-N curve; Weibull distribution; interface crack; recovery of strength*

1. Introduction

Carbon-carbon (C/C) composite was first developed as a heat resistant material to meet the demands that were requested by the reentry mission of a space vehicle from the space[1]. Because of its low density, high melting point, low thermal expansion and high specific stiffness and strength at a high temperature, C/C composite has been used as aircraft and automobile brakes.

Though C/C composite has many advantages as mentioned above, it has a problem of oxidation at high temperatures. If there is no protective coating against the oxidation reactions, C/C composite degrades in air at 550 degrees in centigrade. Another one is its production cost. Both the present production methods, that is, chemical vapor deposition and organic carbonization require long time for production of more than several months, which leads to the high production cost. Metal impregnated C/C composites are produced quickly at low cost compared to both CVD and organic carbonization cases.

It was reported that the tensile fracture occurred at the slot area of a rotor disk developed for the aircraft brake[2]. Generally brake disks are used repeatedly and thus the rotor disk might be damaged due to the tensile cyclic loading. Wang et al. studied the tensile property of these materials[3]. However, the behavior under repeated tensile loading has not been revealed. Thus, tensile cyclic tests were conducted in this study and the cyclic strength and macroscopic failure modes of metal impregnated C/C composites are discussed. Three types of materials, C/C, Cu-C/C and Si-C/C were tested to compare each cyclic strength and mechanism.

*1 Department of Aeronautics and Astronautics, Graduate School of Engineering, Kyushu University
*2 Research Institute for Applied Mechanics, Kyushu University

2. Experimental

2-1 Materials

C/C and metal-impregnated C/C composites used in this study were produced by NGK Insulators, LTD., Japan. The C/C composites were produced by a method called preformed yarn method. First, carbon fibers and carbon binders were put into a 5mm diameter polymer tube, which is called a preformed yarn. Preformed yarns were woven into a "prepreg" sheet with fills. Prepreg sheets were laid up with the cross ply stacking sequence and sintered by a hot press machine. The C/C composite through this novel and economical preformed yarn process has many pores and its density is low. It is improved by impregnating metal into these pores and metal impregnated C/C composites such as Cu-C/C and Si-C/C are produced. Cu- C/C composite with a quick impregnation of Cu under high pressure and temperature is improved in strength, stiffness and wear

Table 1 Material properties of C/C and metal impregnated C/C composites[3)]

Material	Density (g/cm^3)	Porosity (%)	Wear rate ($mm^3/N\ km$)	Ultimate Tensile Strength (MPa)	Stiffness in Tension (GPa)	ILSS (MPa)
C/C	1.70	20	0.77	238	54	4.0
Cu-C/C	2.50	2~3	0.10	279	62	15.4
Si-C/C	2.05	2~3	0.05	55	58	14.1

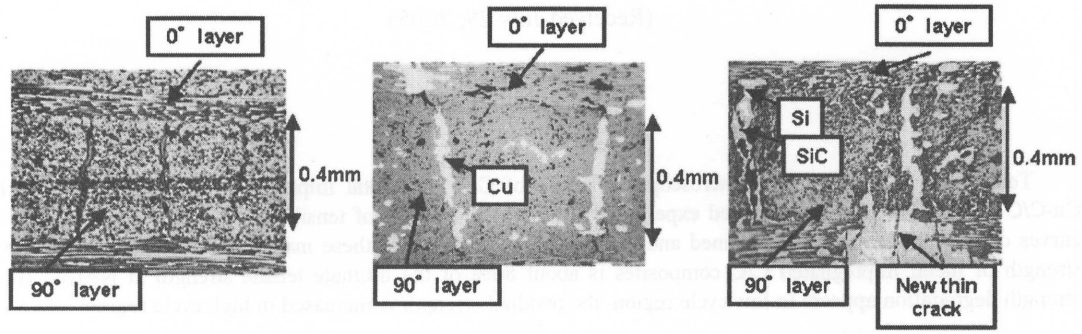

(a) (b) (c)

Fig. 1 Micrographs of C/C and metal impregnated C/C composites: (a) C/C, (b) Cu-C/C, (c) Si-C/C[3)]

property. Si-C/C composite with impregnation of Si under a carefully controlled high temperature is improved in resistance against oxidation and wear. Their material properties are summarized in Table1[3)]. Figs.1 (a), (b) and (c) show micrographs of C/C, Cu-C/C and Si-C/C, respectively. C/C has many pores including cracks in a 90-degree layer and voids in both 0-degree and 90-degree layers and along their boundary as shown in Fig.1 (a). In Fig.1 (b), it is observed that Cu is impregnated into most of these pores. Fig.1 (c) shows that most of pores are filled, a new SiC layer is produced around impregnated Si and new thin transverse cracks are produced perpendicular to the fiber direction in a 0-degree layer. Here, the layer with fibers perpendicular to the cross section is called as a 90-degree one.

Fig.2 shows dimensions of the specimen used in this study, where aluminum tabs are attached to protect the gripped region of specimens against compressive damage. In C/C and Cu-C/C cases, specimens are rectangular, while brittle Si-C/C specimens are waisted to avoid the undesirable fracture at the grip end.

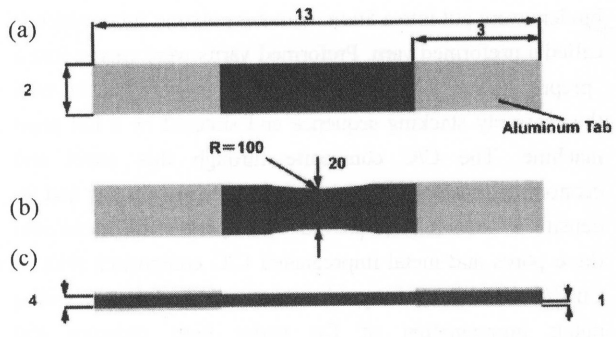

Fig. 2 Dimensions of the specimen in mm: (a) C/C and Cu-C/C, (b) Si-C/C, (c) edge view

2.2 Testing Methods

Strain is measured at a center of the specimen by an extensometer. Cyclic loading tests were conducted in tension-tension mode with a stress ratio R of 0.1 at the frequency of 8Hz using a MTS servo hydraulic testing machine. The maximum tensile stress of cyclic tests was from 75% to 90% of the average ultimate tensile strength (UTS) of the composites and the loading waveform is sinusoidal. The cyclic test was stopped when the specimen was fractured or the number of cycles reached to 10^6. Monotonic tensile loading tests are also performed with the same specimen to obtain UTS and other reference results for discussions.

3. S-N Curves

3.1 Conventional S-N Curve

Fig.3 shows the S-N (stress vs. number of cycles) curve of each material. Straight lines are obtained with the least square method. Resulted lines show that the cyclic strength of these materials at 10^6cycles is about 80% of each UTS. Arrows in the figure mean that the specimen survived after 10^6 cycles. It is observed that the cyclic life of C/C and metal impregnated C/C composites has rather wide distribution. Thus, to assess the dispersion of data seriously, an idea of Weibull distribution is used.

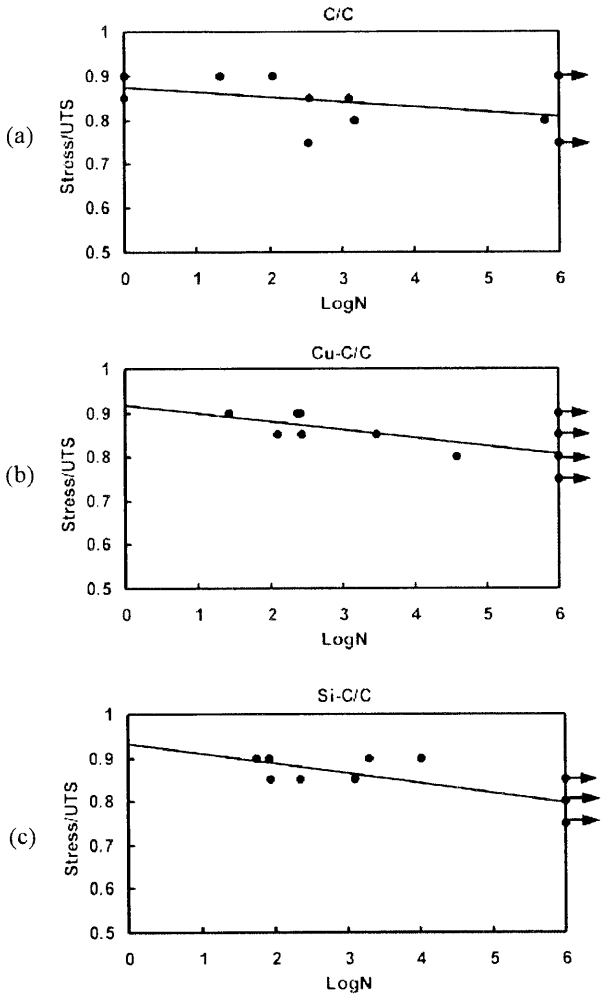

Fig. 3 S-N curve of (a) C/C, (b) Cu-C/C and (c) Si-C/C

3.2 S-N Curve based on Weibull Distribution

The Weibull distribution is a well-established method to assess the reliability of data of cyclic life. The reliability of life exceeding N cycles can be written as[4), 5)]

$$R(N)=\exp\left[-\left(\frac{N}{N_0}\right)^{\alpha_f}\right] \tag{1}$$

using a two-parameter Weibull distribution, where R (N) is the reliability of N (probability of survival at N), N_0 is the characteristic time-to-failure (location parameter) and is the shape parameter.

The Weibull parameters can be estimated using Maximum Likelihood Estimator (MLE). In the high cycle case, censoring technique is also applied. This technique does not require that all specimens fail. Let m be the number of stress level, and n_i the number of specimens tested at the i-th stress level, S_i. The data set can be written as

$$N_i(N_{i1},N_{i2},\ldots,N_{in_i}),\quad i=1,2,\ldots,m \tag{2}$$

The Weibull distribution at each stress level can be written as

$$R(N_i)=\exp\left[-\left(\frac{N_i}{N_{0i}}\right)^{\alpha_{fi}}\right] \tag{3}$$

The likelihood equation with the censoring technique can be written as

$$\frac{\sum_{j=1}^{n} N_{ij}^{\hat{\alpha}_{fi}}\ln N_{ij}+(n_i-r_i)R_i^{\hat{\alpha}_{fi}}\ln R_i}{\sum_{j=1}^{n} N_{ij}^{\hat{\alpha}_{fi}}+(n_i-r_i)R_i^{\hat{\alpha}_{fi}}}-\frac{1}{r_i}\sum_{j=1}^{n}\ln N_{ij}-\frac{1}{\hat{\alpha}_{fi}}=0 \tag{4}$$

$$\hat{N}_{0i}=\left\{\frac{1}{r_i}\left[\sum_{j=1}^{n} N_{ij}^{\hat{\alpha}_{fi}}+(n_i-r_i)R_i^{\hat{\alpha}_{fi}}\right]\right\}^{1/\hat{\alpha}_{fi}} \tag{5}$$

where r_i is the number of cycles at failure under S_i, R_i is the number of cycles at which the test is terminated, and $\hat{\alpha}_{fi}$ and $\hat{N}_{0i}$ mean the estimated values of α_{fi} and N_{0i}, respectively.

In order to determine the shape parameter that α_f is independent of stress level, the data set is normalized as

$$X_i(X_{i1},X_{i2},\ldots,X_{in_i}),\quad i=1,2,\ldots,m \tag{6}$$

where

$$X_{ij}=\frac{N_{ij}}{\hat{N}_{0i}} \tag{7}$$

The Weibull distribution for a normalized data set can be written as

$$R(X)=\exp\left[-\left(\frac{X}{X_0}\right)^{\alpha_f}\right] \tag{8}$$

The likelihood equation with the censoring technique to determine the common shape parameter can be written as

$$\frac{\sum_{i=1}^{m}\sum_{j=1}^{n} X_{ij}^{\bar{\alpha}_f}\ln X_{ij}+\sum_{i=1}^{m}(n_i-r_i)Y_i^{\bar{\alpha}_f}\ln Y_i}{\sum_{i=1}^{m}\sum_{j=1}^{n} X_{ij}^{\bar{\alpha}_f}+\sum_{i=1}^{m}(n_i-r_i)Y_i^{\bar{\alpha}_f}}-\frac{1}{N}\sum_{i=1}^{m}\sum_{j=1}^{n}\ln X_{ij}-\frac{1}{\bar{\alpha}_f}=0 \tag{9}$$

$$\bar{X}_0=\left\{\frac{1}{N}\left[\sum_{i=1}^{m}\sum_{j=1}^{n} X_{ij}^{\bar{\alpha}_f}+\sum_{i=1}^{m}(n_i-r_i)Y_i^{\bar{\alpha}_f}\right]\right\}^{1/\bar{\alpha}_f} \tag{10}$$

where

$$Y_i=\frac{R_i}{\hat{N}_{0i}} \tag{11}$$

and

$$N=\sum_{i=1}^{m} r_i \tag{12}$$

The value $\hat{N}_{0i}$ of can be adjusted as

$$\bar{N}_{0i}=\bar{X}_0\hat{N}_{0i} \tag{13}$$

Assuming a power law representation to describe the S-N

curve for any desired reliability, the S-N curve takes the form

$$CNS^{b} = 1 \tag{14}$$

where b and C are material constants. When $N=N_0$, -ln R $(N_0)=1$, Eq14 can be written with the use of Eq1 as

$$S(N_0) = KN_0^{-1/b} \tag{15}$$

where

$$K = C^{-1/b} \tag{16}$$

A plot of log S versus log N_0 produces a straight line of the characteristic S-N curve with slope $-1/b$ and a y intercept of log K. Using Eqs1 and 15, Eq14 can be written as

$$S = K\left\{\left[-\ln R(N)\right]^{1/\alpha_f b}\right\}N^{-1/b} \tag{17}$$

With K, b, and α_f determined, Eq17 can be used to produce a S-N curve with any desired reliability.

Fig.4 shows the characteristic S-N (being nearly equal to mean time-to-failure) and 95% survivability curves of each material calculated from Eq15 and Eq17, respectively. The solid dots denote experimental data and the stress is normalized by each UTS designated as S_0 here. In general, the 95% survivability curve is used to assess the reliability of cyclic life. Normalized curves of three materials describe that the survivability and characteristic strength at 10^6 cycles are about 60% and 80% of UTS, respectively, in all materials. The difference of survivability is small, that is, survivability is not radically affected by metal impregnation.

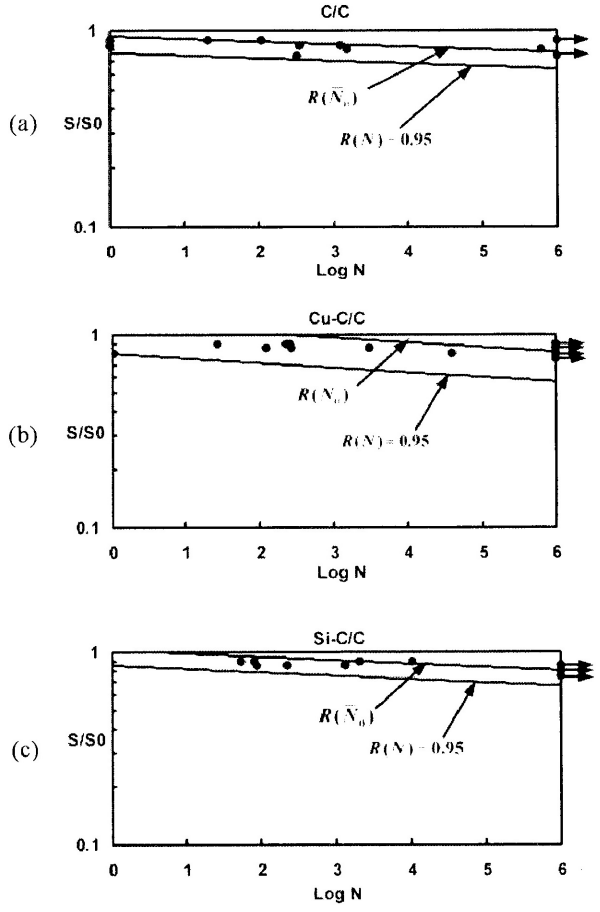

Fig. 4 Characteristic S-N curve and 95% survivability curve of of (a) C/C, (b) Cu-C/C and (c) Si-C/C

4. Fracture Morphology

Fig.5 shows the fracture morphology of (a) C/C, (b) Cu-C/C and (c) Si-C/C specimens. Delamination between 0 and 90-degree layers is noticed in the large area of C/C as shown in Fig. 5 (a). The color is gray while the original surface is in black. Though the same kind of delamination to the C/C case is also observed in Cu-C/C, the area of delamination is smaller than the C/C case. In Si-C/C delamination as in C/C is not detected but the localized brittle fracture is a primary failure mode.

Difference of the failure mechanism between C/C, Cu-C/C and Si-C/C can be explained by both their interlaminar shear strength (ILSS) and UTS. Table 1 shows that ILSS of C/C is the lowest among three and it is reasonable to consider that delamination occurs easily in C/C. In Cu-C/C there is about 20 and 250% increases of UTS and ILSS, respectively, compared to the C/C case. The increases of UTS and ILSS make fracture modes into delamination and tension, respectively. In Cu-C/C, the 250% increase of ILSS effectively decreases the area of delamination. In Si-C/C, though ILSS is almost the same to the Cu-C/C case, UTS of Si-C/C is less than 20% of the Cu-C/C case and the tensile fracture mode can be active. A rather small change of fracture mode in Cu-C/C is a result of balance due to the negative effect to the change by the increase of UTS and positive effect by the increase of ILSS. On the other hand, the drastic change of fracture mode to brittle tensile fracture in Si-C/C is due to both positive effects by the decrease of UTS and increase of ILSS.

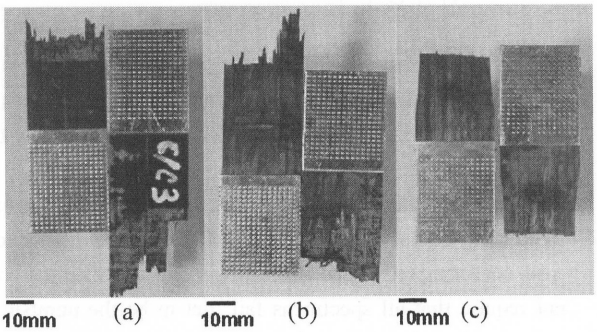

Fig. 5 Fractured specimens: (a) C/C with 0.8UTS and $N=1.524\times10^3$, (b) Cu-C/C with 0.9UTS and $N=2.60\times10^2$, (c) Si-C/C with 0.85UTS and $N=1.307\times10^3$

5. Cyclic Stress Strain Curve

Fig.6 (a)~(c) shows stress-strain curves of (a) C/C, (b) Cu-C/C and (c) Si-C/C under the specific maximum stress σ_{max}=0.8UTS, 0.9UTS and 0.85UTS, respectively. Fig.6 (d) shows variation of elastic modulus. Fig.6 (b) and (c) clearly show that there is hysteresis in the stress-strain relationship, which verifies the existence of energy dissipation process within a single cycle. Moreover, the gradient of each curve is gradually decreased with N increasing, which means that the aforementioned energy dissipation process decreases the rigidity of the specimen. To decrease the rigidity, some kind of propagation or additional initiation of damage such as debonding between fiber and matrix, delamination, void or crack is necessary as a function of N. The damage might not be practical but effective one that could be represented by debonding, delamination, void or crack at the corresponding location or area.

Almost the same magnitude of increase of residual strain is observed in both impregnated Cu-C/C and Si-C/C cases, while it is small in C/C that needs a large number of cycles to yield even the smaller residual strain. Impregnation of metal into the pore increases the stiffness not only just through the occupation by metal but also through the prevention of fibers from moving under small restrictive forces. In Cu-C/C the impregnated Cu under high-pressure compresses C/C (fiber and matrix) around Cu and in Si-C/C resulted hard SiC connects Si and C/C (fiber and matrix), which increases ILSS of both materials. If the slip between layers occurs under the shear stress beyond ILSS, it is just a slip and ILSS does not decrease so much in Cu-C/C. However, ILSS of Si-C/C decreases since the slip occurs by the failure of SiC phase occupying the void at the interface. In Cu-C/C it accompanies the failure or abrasion of Cu. Cu impregnated into voids under high pressure also makes the contact between fiber and matrix next to void more smooth and higher tensile strength of Cu-C/C more than C/C has been achieved.

Though hysteresis in a single cycle is small and the gradient of curves is practically constant in C/C, the increase of residual strain is clearly observed. Roughly the linear stress strain curve moves a little along the loading direction with no change of gradient. To achieve this behavior the interaction between 0 and 90 degree layers has to be quite small and the tensile load be supported mainly by fibers in 0 degree layers. Microscopically the constraint by the matrix to a fiber has to be also small. Then, even if there appears delamination or debonding that yields small residual strain and decrease of stiffness, stiffness is recovered by the nonlinear increase of stiffness due to the easy rotation of fiber direction to the loading axis.

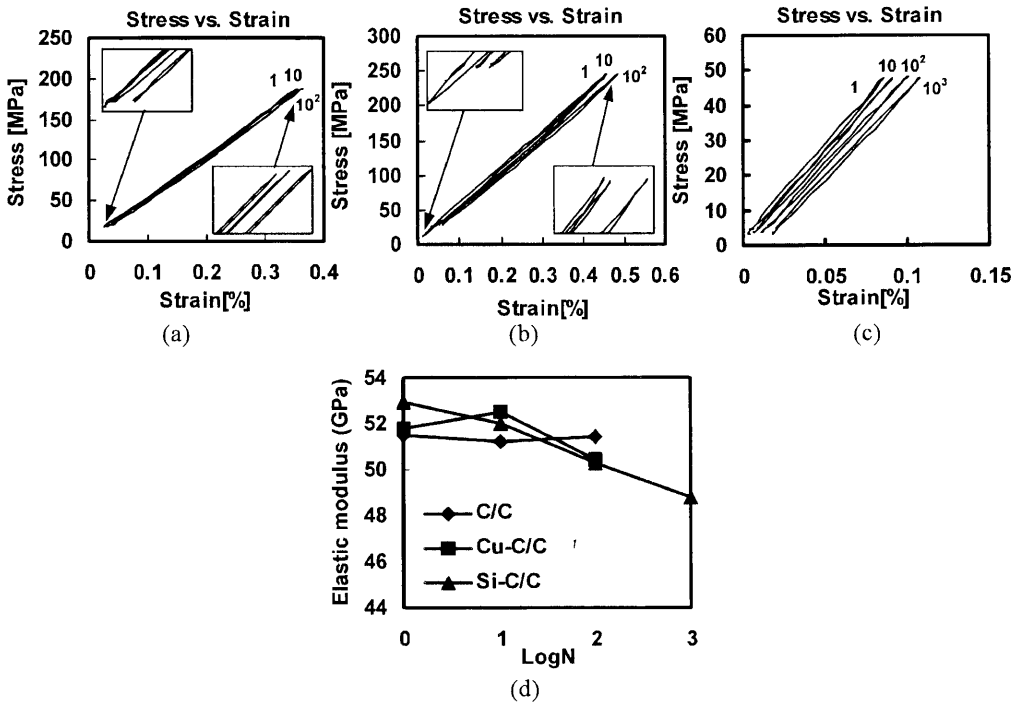

Fig.6 Stress-strain curves of (a) C/C with 0.8UTS and N=1.524x10^3, (b) Cu-C/C with 0.9UTS and N=2.60x10^2 and (c) Si-C/C with 0.85UTS and N=1.307x10^3, (d) variation of elastic modulus

6. Other Characteristics

Fig.7 shows optical photographs of C/C specimens under both (a) cyclic and (b) monotonic tensile loading conditions. In both C/C and Cu-C/C cases, it is observed that delamination area of fatigue specimen is larger than that of tensile specimen. In Si-C/C, delamination is not detected practically under either loading condition. Macroscopic deformation or damage is reduced in fatigue failure in the present materials.

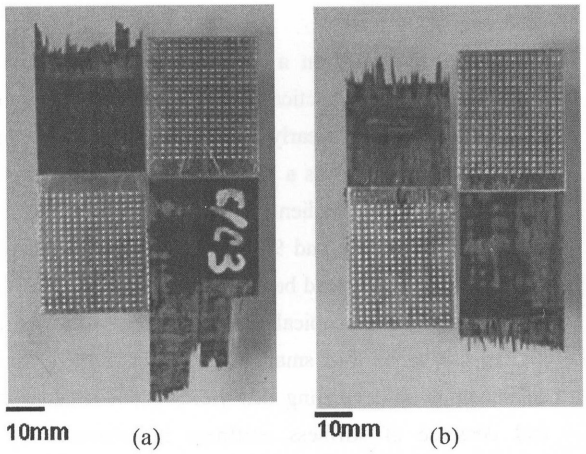

Fig.7 Fractured specimens of C/C under (a) cyclic loading with 0.8UTS and N=1.524x10^3 and (b) monotonic loading

The residual tensile strength of survived specimens after 10^6 cycles' run was measured. Average residual strength is shown in Table 2 and is higher than UTS in every material. In addition, most of fatigue fracture occurs less than 10^4 cycles. The same results were obtained in C/C[6], which means that the effect of interfacial crack in low cycle region is different from the high cycle case.

Table 2 Residual strength of C/C and metal impregnated C/C composites at N= 10^6

Material	Average Residual Strength (MPa)	UTS (MPa)
C/C	265	238
Cu-C/C	286	279
Si-C/C	64	55

7. Conclusions

1. C/C and metal impregnated Cu-C/C and Si-C/C based on a preformed yarn method are loaded cyclically in tension and tension and it is found that they have fatigue property with S-N curves.
2. The cyclic strength at 10^6 cycles is about 80% of each UTS in all materials and the normalized cyclic strength is not radically affected by metal impregnation into C/C composites.
3. Stress strain curves as a function of number of cycle N show that there are hysteresis loop in each material, decrease of stiffness, that is damage propagation in Cu-C/C and Si-C/C, and increase of residual strain with N increasing for three materials.
4. In C/C and Cu-C/C delamination appears, while local brittle fracture occurs without practical delamination in Si-C/C. Though ILSS of Cu-C/C is high and almost the same to Si-C/C, delamination appears in Cu-C/C. These characteristics are explained by UTS and ILSS.
5. Average residual strength is higher than UTS in every material and most of fatigue fracture occurs less than 10^4 cycles.

References

1) D.M. Curry, J.W. Latchem and G.B. Whisenhunt, Space Shuttle Orbiter Leading Edge Structural Subsystem Development, AIAA-83-0483, 1983.
2) J.S. Yoo, D.U. Sung, C.G. Kim, C.S. Hong and K.S. Kim, Mechanical strength experiments of carbon/carbon brake disk, Proceedings of ACCM-2000, pp.715-720, 2000.
3) W.X. Wang, K. Iihoshi, T. Matsubara and Y. Takao, Tensile properties of C/C and metal impregnated C/C composites, Proceedings of ICCM13, Beijing, ID=1432, 2001.
4) H.T. Hahn, Fatigue of composites, in: Delaware Composites Design Encyclopedia: Mechanical Behavior and Properties of Composite Materials, Vol.1, pp.73-130, 1989.
5) J.M. Whitney, Fatigue characterization of composite materials, in: Fatigue of Fibrous Composites, ASTM STP 723, pp.133-151, 1981.
6) K. Goto, H. Hatta and D.Katsu, Tensile fatigue of a laminated carbon-carbon composite at room temperature, Carbon, 41, pp.1249-1255, 2003